THE ASTRONOMICAL JOURNAL, 119:2540–2555, 2000 June

THE ASIAGO-ESO/RASS QSO SURVEY. I. THE CATALOG AND THE LOCAL QSO LUMINOSITY FUNCTION[1]

A. GRAZIAN
Department of Astronomy, University of Padua, I-35122 Padua, Italy

S. CRISTIANI[2]
European Southern Observatory, Space Telescope European Coordinating Facility, Karl-Schwarzschild-Strasse 2, Garching bei München, D-85748 Germany

V. D'ODORICO
International School for Advanced Studies, Astrophysics Sector, via Beirut 4, Trieste, I-34013 Italy

A. OMIZZOLO
Vatican Observatory Research Group, Steward Observatory, University of Arizona, 933 North Cherry Avenue, Tucson, AZ 85721

AND

A. PIZZELLA
European Southern Observatory, St. Alonso de Cordova 3107, Vitacura, Casilla 19001, Santiago 19, Chile and Department of Astronomy, University of Padua, I-35122 Padua, Italy

Received 1999 November 12; accepted 2000 February 16

ABSTRACT

This paper presents the first results of a survey for bright quasars ($V < 14.5$ and $R < 15.4$) covering the northern hemisphere at Galactic latitudes $|b| > 30°$. The photometric database is derived from the Guide Star and USNO catalogs. Quasars are identified on the basis of their X-ray emission measured in the *ROSAT* All-Sky Survey. The surface density of quasars brighter than 15.5 mag turns out to be $(10 \pm 2) \times 10^{-3}$ deg^{-2}, about 3 times higher than that estimated by the PG survey. The quasar optical luminosity function (LF) at $0.04 < z \leq 0.3$ is computed and shown to be consistent with a luminosity-dependent luminosity evolution of the type derived by La Franca & Cristiani in the range $0.3 < z \leq 2.2$. The predictions of semianalytical models of hierarchical structure formation agree remarkably well with the present observations.

Key word: galaxies: clusters: general

1. INTRODUCTION

Quasar surveys provide basic information for understanding a number of astrophysical, cosmological, and cosmogonical issues: the formation and evolution of galactic structures, the physics of the active galactic nucleus (AGN) phenomenon, and the UV and X-ray backgrounds. The general behavior of the quasi-stellar object (QSO) optical luminosity function (OLF) is well established in the redshift interval $0.3 < z < 2.2$, for which color techniques provide reliable selection criteria (for a review of the subject, see Hartwick & Schade 1990; Boyle 1992; Hewett & Foltz 1994). A pure luminosity evolution (PLE) appears to describe the data in the interval $0.6 < z < 2.2$ reasonably well. In the range $0.3 < z < 0.6$, the OLF appears to be flatter than observed at higher redshifts (Goldschmidt et al. 1992), requiring a luminosity-dependent luminosity evolution (LDLE; La Franca & Cristiani 1997, hereafter LC97). This departure from a PLE provides an interesting clue for the physical interpretation of the QSO evolving population (Cavaliere, Perri, & Vittorini 1997; LC97). The present observational evidence, however, relies on a relatively small number of objects: in the $0.3 < z < 0.6$ range for $M_B < -25$, 32 QSOs are observed by LC97 instead of the 19 expected from the best-fit PLE model. Analogous results by Köhler et al. (1997) and Goldschmidt & Miller (1998) are likewise based on very small samples.

To provide a statistically solid basis for the LDLE pattern and to investigate whether such a trend persists (and possibly becomes more evident) at redshifts lower than 0.3, we decided to carry out a new large-area survey of quasars at bright optical fluxes. A typical apparent magnitude for an $M_B = -24$ QSO at $z \sim 0.1$ is in fact $B \sim 14.5$, and the surface density of these objects, according to previous surveys (e.g., the Palomar Bright Quasar Survey [BQS]; Schmidt & Green 1983), is expected to be less than 10^{-3} deg^{-2}, requiring an efficient selection criterion and coverage of a significant fraction of the whole sky to collect a meaningful sample.

In § 2, we describe the photometric database from which optical fluxes have been derived; in § 3, the criteria followed to select the candidates; in § 4, the spectroscopic follow-up; in § 5, the derived quasar counts and the optical luminosity function; and in § 6, a few consequences for model scenarios.

2. PHOTOMETRIC DATABASE

A number of photometric catalogs are available in the literature, covering a substantial fraction of the celestial sphere down to the optical magnitudes of interest for the present survey. We have chosen the USNO (Monet et al. 1996), GSC (Lasker et al. 1988), and the DSS (Digitized Sky Survey[3]).

To test the accuracy of the photometric calibration of these catalogs, we have used as a comparison in the north-

[1] Based on material collected with the ESO-La Silla, Asiago, NOAO, and VATT telescopes.

[2] On leave from the Department of Astronomy, University of Padua.

[3] See http://arch-http.hq.eso.org/dss/dss.

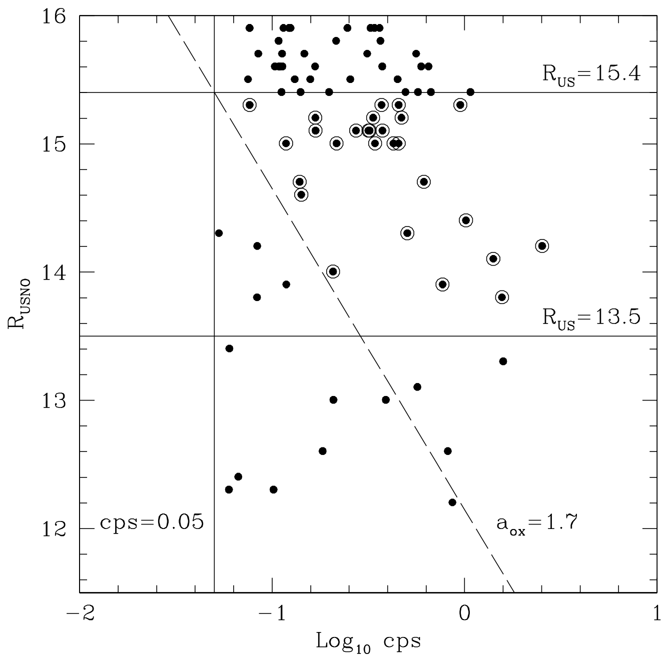

FIG. 1.—Incompleteness in the present selection of quasar candidates, due to objects not found in the RASS catalog (with flux ≤ 0.05 cps, on the left of the vertical line) and to the ones with $\alpha_{ox} \geq 1.7$ (on the left of the dashed line).

ern sky the photometric standards of Landolt (1992). In the southern hemisphere, we have used 446 standards derived from the input catalog used to calibrate the photometric material of the Homogeneous Bright Quasar Survey (HBQS; Cristiani et al. 1995). From both samples only relatively bright ($12.5 \leq V \leq 16.0$) and not too red ($B-R \leq +1.0$) stars have been chosen to match the characteristics of the quasars searched for in this survey.

We finally defined three flux-limited samples, adopting the following photometric references:

1. In the northern hemisphere, objects with $11.0 < V_{GSC} \leq 14.5$ in the GSC catalog. The relation between the V_{GSC} band and the corresponding Johnson V band turned out to be

$$V_{GSC} = V - 0.21 , \quad (1)$$

with $\sigma_V = 0.27$ mag. Seven (4%) of the 183 Landolt stars used for this comparison were not found in the GSC catalog.

2. In the northern hemisphere, objects from the USNO catalog with $13.5 < R_{USNO} \leq 15.4$. The relation between the R_{USNO} band and the corresponding Johnson-Kron-Cousins R band turned out to be

$$R_{USNO} = R_{JKC} + 0.096 , \quad (2)$$

with $\sigma_{R_{USNO}} = 0.267$ mag. No correlation between the residuals of $R_{USNO} - R_{JKC}$ and the color $(B-R)_{JKC}$ has been found. According to Monet et al. (1996), the internal magnitude estimators for stars in the USNO catalog are probably accurate to something like 0.15 mag over the range from $R_{USNO} = 12$ mag to 19 mag, but the systematic error arising from the plate-to-plate differences is at least 0.25 mag in the northern hemisphere, consistent with our estimates.

3. In the southern hemisphere, we have derived B_J magnitudes from the Digitized Sky Survey (DSS). Small scans ("postage stamps" of area $2' \times 2'$) of each object of interest and of 20–50 surrounding objects with known GSC B_J magnitudes were extracted from the DSS. The magnitude of the object of interest was then calibrated against the GSC objects. In this way a σ_{B_J} of 0.10 mag was obtained in the interval $12.0 < B_J < 15.5$.

3. SELECTION OF THE SAMPLE

3.1. *ROSAT All-Sky Survey*

To pick out the bright quasars from the overwhelming number of stars in the same magnitude range, an efficient selection criterion is required. A convenient possibility is offered by the X-ray emission, which is a key signature of the AGN phenomenon. The *ROSAT* All-Sky Survey (Voges 1992, hereafter RASS) was carried out during the period 1990 July to 1991 February with the Position Sensitive Proportional Counter (PSPC) and has produced a photometric database in the soft X-ray band (0.1–2.4 keV). This shallow survey covers almost the entire sky at a bright level (10^{-13} ergs cm^{-2} s^{-1}) and initially contained 60,000 sources. A more evolved reduction analysis, SASS-II, has produced the RASS Bright Source Catalog (RASS-BSC; Voges et al. 1999), a sample of 18,811 X-ray sources at a limiting flux level of 0.05 cps all over the sky.[4]

The main constituents of the RASS catalog are AGNs and peculiar stars (cataclysmic variables, M stars, K stars, WDs, X-ray binaries, and coronally active stars), but there are also clusters of galaxies, BL Lacertae objects, supernova remnants, neutron stars, and normal galaxies (or starbursts). A convenient way to distinguish and isolate AGNs is the comparative analysis of their soft X-ray and optical properties (Hasinger et al. 1998).

We have cross-correlated the RASS catalog with the photometric databases described in the previous section for sources at Galactic latitudes $|b| \geq 30°$ and with an RASS-BSC exposure time $\geq$300 s, i.e., flux $\leq$0.05 cps. Sources classified as extended in the RASS have been disregarded, while no selection based on optical morphology was applied. We have looked for optical objects in the ranges $11.0 < V_{GSC} \leq 14.5$ and $13.5 < R_{USNO} \leq 15.4$ around the

[4] The unit cps is counts per second and is a measure of the flux of a source when a precise soft X-ray spectrum is considered. For $F(\nu) \propto \nu^{-1}$, the value 0.05 cps corresponds to 10^{-13} ergs s^{-1} cm^{-2}.

TABLE 1

SELECTION CRITERIA AND COMPLETENESS

Subsample	Magnitude Interval	α_{ox} (max)	Completeness (N_{found}/N_{VV98})	Completeness (Percent)
USNO……	$13.5 < R < 15.4$	1.7	24/36	68
GSC……..	$12.5 < V < 14.5$	1.9	5/8	63
DSS………	$12.6 < B_J < 15.2$	1.9	8/9	89

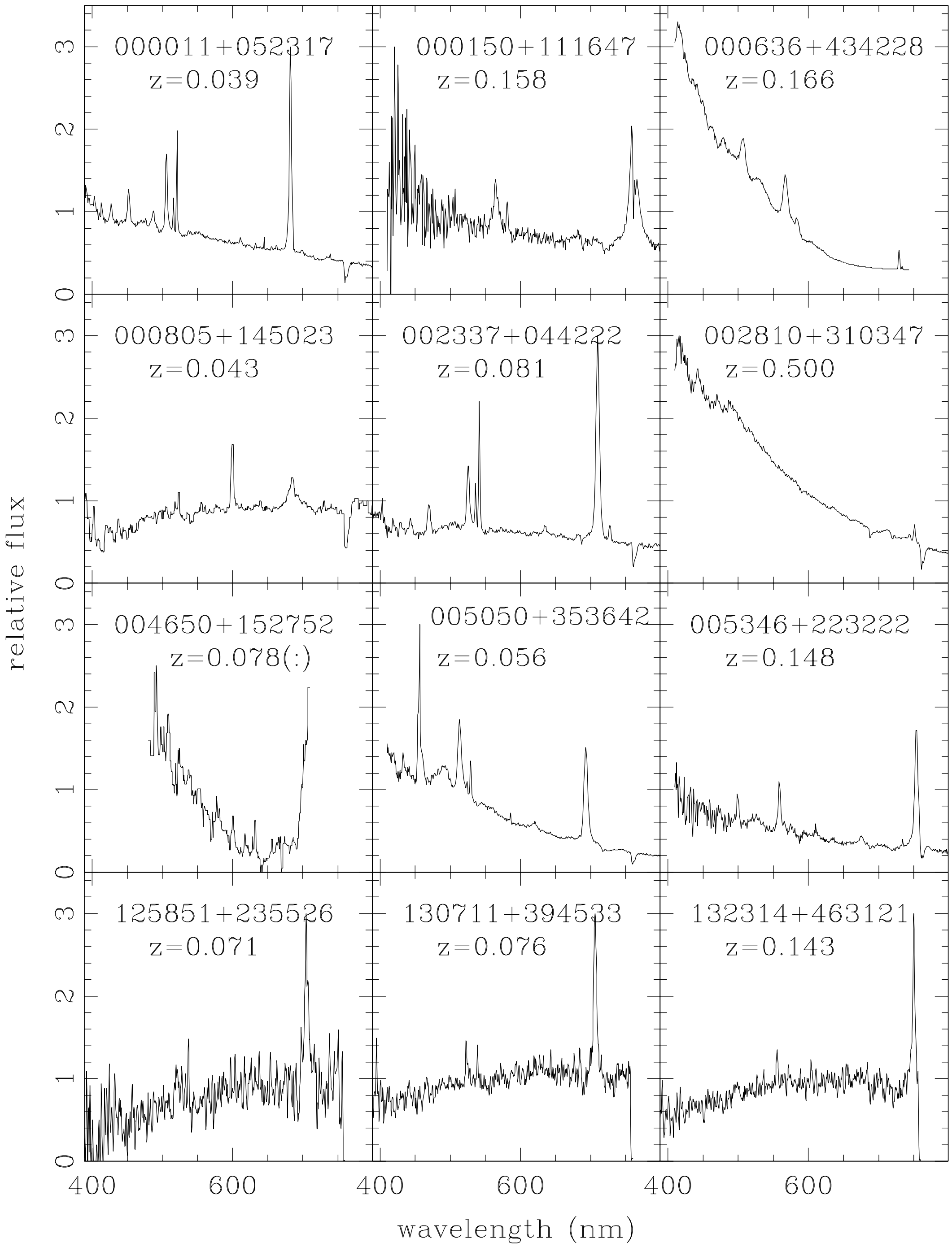

FIG. 2*a*

FIG. 2.— Spectra of the AGNs confirmed with the follow-up spectroscopy

RASS sources, adopting a matching radius 3 times the rms positional uncertainty of each entry in the RASS catalog (typically $3 \times 12''$). In this way, very few (of the order of 0.1%) true identifications in the desired optical range are missed. Misidentifications, i.e., "X-ray–quiet" AGNs in the desired optical magnitude range falling by chance in the RASS error box, are also possible but extremely unlikely, given the low surface density of these bright AGNs, and are in any case irrelevant for the present work, which aims at the definition of the local *optical* QSO LF. The resulting catalog covers 8164 deg^2 in the north and 5855 deg^2 in the south.

3.2. *The α_{ox} Distribution of Quasars and the Selection Criteria*

For each source, the α_{ox} index was computed as $\alpha_{ox} = -0.408 \log(\text{cps}) - 0.163R + 3.65$, $\alpha_{ox} = -0.428 \log(\text{cps}) - 0.171V + 3.84$, or $\alpha_{ox} = -0.483 \log(\text{cps}) - 0.193B_J + 4.20$. To obtain an estimate of the intrinsic distribution of the α_{ox} of quasars, we have plotted the observed B, V, and R magnitudes versus the log(cps) for the $0.04 < z \leq 0.3$ quasars listed in the eighth edition of the Véron catalog (1998, hereafter VV98). Figure 1 shows the result for northern QSOs and R magnitudes.

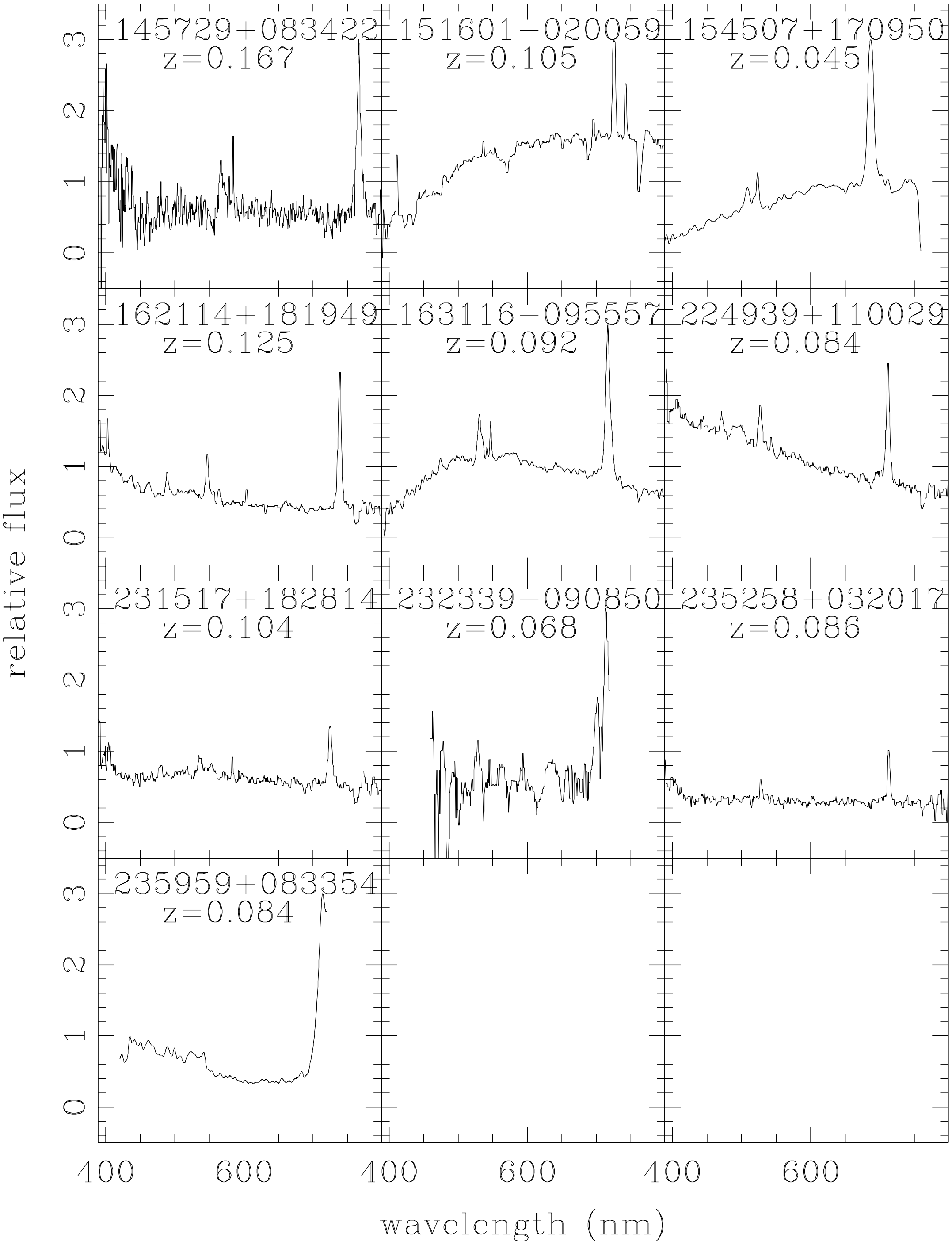

FIG. 2*b*

In this diagram, the locus α_{ox} = const is represented by a diagonal line. X-ray–quiet objects, i.e., those for which flux ≤ 0.05 cps (to the left of the vertical line in Fig. 1), are missed in the RASS. If we assume that the intrinsic distribution of the α_{ox} is not a function of the apparent luminosity (Yuan, Siebert, & Brinkmann 1998), selecting objects with $\alpha_{ox} < \alpha_{max}$ (i.e., X-ray loud) that are optically brighter than a convenient limit will provide a sample with a degree of incompleteness that is not a function of the apparent magnitude. For example, in the case of the USNO database the limit in R turns out to be $R < [3.65 - \alpha_{max} - 0.408 \log(\mathrm{cps_{min}})]/0.163 = 25.64 - 6.13\alpha_{max}$. If we adopt (see Fig. 1) an $\alpha_{max} = 1.7$ at magnitudes brighter than $R = 15.4$, only the objects with $\alpha_{ox} > \alpha_{max}$ will be missed.

Table 1 lists the interval of optical magnitudes and the corresponding limit on α_{ox} chosen for the USNO, GSC, and DSS subsamples. The last column shows the degree of completeness estimated on the basis of the fraction of quasars of the VV98 found with the adopted criterion.

Examining the properties of the VV98 quasars in terms of the various RASS parameters, we have found two further empirical criteria, based on the hardness ratios HR1 and HR2 (Voges et al. 1999), to increase the effectiveness of the selection without affecting its completeness:

TABLE 2

USNO SAMPLE

Name (1RXS)	R.A. (J2000.0)	Decl. (J2000.0)	R_{USNO}	V_{GSC}	z	Type
J000150.9+111705......	00 01 50.6	+11 16 47.6	15.10		0.158	AGN
J001031.3+105832......	00 10 31.0	+10 58 29.6	13.60	14.66	0.089	AGN
J002337.1+044220......	00 23 37.2	+4 42 22.3	14.30	15.13	0.081	AGN
J002811.6+310342......	00 28 10.8	+31 03 47.8	15.30		0.500	AGN
J002913.9+131605......	00 29 13.7	+13 16 03.6	15.30	15.23	0.142	AGN
J004240.8+301742......	00 42 41.6	+30 17 43.9	14.40			
J005154.8+172552......	00 51 54.8	+17 25 58.4	15.30		0.064	AGN
J013556.7+231605......	01 35 58.5	+23 15 56.5	15.20			
J013624.3+205712......	01 36 25.3	+20 56 49.6	14.70			
J014239.9+000514......	01 42 38.4	+0 05 14.9	15.30			
J015242.1+010040......	01 52 41.9	+1 00 25.1	14.40	13.57	0.230	Gal
J015524.9+022818......	01 55 24.9	+2 28 16.2	15.10			
J015546.4+071902......	01 55 46.4	+7 19 03.8	15.40			
J015935.1+104707......	01 59 34.9	+10 46 46.7	15.20			
J075704.9+583245......	07 57 06.2	+58 32 58.7	14.50	14.48		
J080132.3+473618......	08 01 32.0	+47 36 15.8	15.20		0.158	AGN
J080525.8+753424......	08 05 23.7	+75 34 34.7	15.30	14.40		
J080534.6+543132......	08 05 34.8	+54 31 30.3	14.90			
J080649.5+751853......	08 06 48.3	+75 18 30.7	15.10			
J080938.9+754851......	08 09 39.8	+75 48 55.1	14.20		0.094	AGN
J080949.2+521855......	08 09 49.2	+52 18 58.2	14.50	14.84	0.138	BL
J081059.0+760245......	08 10 58.6	+76 02 42.5	14.20	14.59	0.100	AGN
J081228.3+623627......	08 12 28.2	+62 36 23.3	14.50	14.15		
J083045.0+340527......	08 30 45.4	+34 05 31.6	15.30		0.063	AGN
J083121.0+483148......	08 31 22.3	+48 32 13.9	15.10	15.13		
J083821.6+483800......	08 38 22.0	+48 38 01.7	14.80	14.63		
J084255.9+292752......	08 42 56.0	+29 27 26.2	15.40		0.193	Gal
J084445.2+765313......	08 44 45.3	+76 53 09.3	13.90	15.72	0.131	AGN
J084658.3+704452......	08 47 05.7	+70 44 41.1	15.20	14.62		
J085343.5+574846......	08 53 44.1	+57 48 41.3	15.00		0.000	Star
J085358.8+770054......	08 53 59.4	+77 00 54.6	15.40			
J085823.0+520533......	08 58 24.2	+52 05 40.7	15.10			
J085902.0+484611......	08 59 02.9	+48 46 09.0	14.30	14.99	0.083	AGN
J090020.1+503143......	09 00 19.1	+50 31 40.5	15.10	14.91		
J090038.4+411409......	09 00 38.5	+41 13 55.9	15.10			
J090808.7+500912......	09 08 08.8	+50 09 20.0	15.10			
J090950.6+184956......	09 09 50.6	+18 49 47.6	15.30			
J091010.2+481317......	09 10 10.0	+48 13 41.4	14.30		0.118	AGN
J091254.7+793731......	09 12 49.4	+79 37 51.8	14.70	15.59		
J091552.3+090056......	09 15 51.8	+9 00 50.9	14.50	12.99	0.000	Star
J091651.8+523829......	09 16 52.0	+52 38 27.9	15.30		0.190	BL
J091904.6+732334......	09 19 08.8	+73 23 59.2	15.30			
J091954.9+552120......	09 19 55.3	+55 21 36.6	14.90		0.123	AGN
J092246.4+512046......	09 22 48.0	+51 20 45.9	14.40	14.80		
J092916.4+501344......	09 29 15.7	+50 14 15.7	15.20	13.78		
J093047.9+404446......	09 30 47.8	+40 44 41.3	15.30			
J093355.6+141932......	09 33 55.9	+14 19 19.9	15.40			
J093427.2+745123......	09 34 28.4	+74 51 19.9	14.20			
J093701.0+010548......	09 37 01.0	+1 05 43.0	13.60	13.87	0.051	AGN
J093942.8+560247......	09 39 43.8	+56 02 30.6	14.10		0.116	AGN
J094617.2+025505......	09 46 16.9	+2 54 58.7	15.10			
J094653.0+132000......	09 46 52.6	+13 19 53.6	15.20			
J094713.2+762317......	09 47 16.7	+76 23 28.2	15.00	14.79		
J095104.2+192531......	09 51 03.5	+19 25 32.1	15.30			
J095406.7+212250......	09 54 08.1	+21 22 25.5	14.90			
J095652.4+411524......	09 56 52.3	+41 15 22.3	15.40	15.00		
J095708.1+243319......	09 57 07.2	+24 33 15.6	14.50			
J100050.9+315555......	10 00 52.1	+31 56 03.3	15.20			
J100121.5+555351......	10 01 20.8	+55 53 52.8	14.80		1.414	AGN
J100335.1+444422......	10 03 35.0	+44 44 39.6	15.20			
J100505.4+562426......	10 05 06.1	+56 24 29.3	14.80			
J100659.7+673249......	10 07 00.8	+67 32 46.8	14.00	14.69		
J100851.6+541451......	10 08 54.7	+54 14 45.9	15.40			
J100947.3+523442......	10 09 48.5	+52 34 51.2	15.20			

TABLE 2—*Continued*

Name (1RXS)	R.A. (J2000.0)	Decl. (J2000.0)	R_{USNO}	V_{GSC}	z	Type
J101238.4+101722......	10 12 38.5	+10 17 18.8	14.80			
J101303.2+355131......	10 13 03.2	+35 51 23.3	14.60	15.26	0.070	AGN
J101504.3+492604......	10 15 04.1	+49 25 59.9	15.20		0.200	BL
J101624.0+333827......	10 16 22.9	+33 38 17.0	14.10			
J101645.9+421024......	10 16 45.1	+42 10 25.1	13.90		0.054	AGN
J101702.4+390256......	10 17 03.6	+39 02 49.4	14.30		0.206	Gal
J101716.7+051145......	10 17 16.8	+5 11 49.5	15.00			
J101906.8+231846......	10 19 06.7	+23 18 37.0	15.20			
J102236.0+301753......	10 22 37.4	+30 17 49.8	14.50	14.71		
J102258.8+202252......	10 22 58.2	+20 22 37.5	15.10		0.129	Gal
J102338.5+523356......	10 23 39.6	+52 33 49.4	15.20			
J102531.2+514039......	10 25 31.2	+51 40 34.7	13.60		0.045	AGN
J102836.6+630255......	10 28 37.2	+63 02 48.2	15.00			
J102915.4+572402......	10 29 14.8	+57 23 53.1	15.30		0.186	AGN
J102946.7+401914......	10 29 46.8	+40 19 13.6	14.70	15.07		
J103134.2+284711......	10 31 34.3	+28 47 00.6	15.20		0.060	AGN
J103244.5+391331......	10 32 44.2	+39 13 22.6	15.30			
J103422.3+605316......	10 34 24.9	+60 53 11.5	15.40			
J103439.8+281755......	10 34 39.9	+28 17 41.6	14.80			
J104043.6+330057......	10 40 44.0	+33 00 59.5	14.90		0.081	AGN
J104303.0+005423......	10 43 02.5	+0 54 17.9	14.80			
J104346.6+223006......	10 43 47.0	+22 29 57.4	14.60			
J104427.6+271813......	10 44 27.7	+27 18 05.4	14.00			
J104427.6+271813......	10 44 27.7	+27 18 05.4	14.00			
J104819.1+521837......	10 48 18.0	+52 18 30.3	14.70			
J104926.1+245134......	10 49 25.5	+24 51 23.0	14.70			
J105037.1+801204......	10 50 35.6	+80 11 50.7	14.90	14.85		
J105124.8+382053......	10 51 24.5	+38 20 46.7	15.20			
J105143.8+335936......	10 51 43.8	+33 59 26.5	15.10		0.167	AGN
J105151.0+213739......	10 51 51.0	+21 37 25.9	14.20			
J105214.2+055514......	10 52 15.3	+5 55 08.2	15.00	13.96		
J105355.0+661209......	10 53 55.7	+66 12 01.8	15.30			
J105444.4+483145......	10 54 44.7	+48 31 38.8	15.40		0.286	AGN
J105519.1+402739......	10 55 19.5	+40 27 16.6	15.20		0.120	AGN
J105837.5+562816......	10 58 37.7	+56 28 11.4	14.10		0.144	BL
J110237.0+724633......	11 02 38.3	+72 46 20.7	15.10			
J110412.4+765859......	11 04 13.8	+76 58 58.2	15.40		0.313	AGN
J110537.4+585128......	11 05 37.6	+58 51 20.7	15.20			
J110748.8+710538......	11 07 52.2	+71 06 01.4	14.40	14.75		
J110831.9+695129......	11 08 26.9	+69 51 41.7	15.00			
J111011.4+011333......	11 10 12.1	+1 13 27.2	14.50	15.06		
J111422.6+582318......	11 14 21.9	+58 23 19.0	14.70		0.206	Gal
J111830.0+402557......	11 18 30.4	+40 25 54.5	14.40		0.154	AGN
J111907.1+413018......	11 19 07.6	+41 30 03.0	15.40			
J112034.0+100821......	11 20 34.2	+10 08 04.5	15.20			
J112147.3+114420......	11 21 47.1	+11 44 18.2	13.50	14.48	0.050	AGN
J112349.2+723002......	11 23 51.8	+72 30 08.4	15.00	15.09		
J112842.9+633559......	11 28 41.6	+63 35 50.5	15.40			
J112850.7+231036......	11 28 51.1	+23 10 37.0	15.40			
J112854.0+210630......	11 28 55.2	+21 06 30.9	15.30			
J113109.0+263212......	11 31 09.3	+26 32 07.8	15.40			
J113302.0+184655......	11 33 02.0	+18 47 32.8	15.20			
J113313.3+500837......	11 33 12.7	+50 08 56.6	15.00		0.310	Gal
J113630.9+673708......	11 36 30.1	+67 37 04.0	15.40		0.135	BL
J113737.4+103931......	11 37 38.1	+10 39 30.2	15.30			
J113826.8+032210......	11 38 27.1	+3 22 09.9	14.90			
J113849.7+574245......	11 38 49.6	+57 42 43.9	13.60		0.115	AGN
J114009.0+030727......	11 40 08.7	+3 07 11.0	15.30			
J114106.1+024110......	11 41 05.7	+2 41 16.3	15.10			
J114247.5+215717......	11 42 45.8	+21 57 22.4	15.30	13.25		
J114509.2+381326......	11 45 09.9	+38 13 29.1	15.40			
J114509.3+304724......	11 45 10.3	+30 47 16.7	14.30		0.059	AGN
J114606.1+035959......	11 46 06.2	+3 59 55.2	14.60			
J114755.3+090235......	11 47 55.0	+9 02 28.6	14.50			
J115137.3+561341......	11 51 38.1	+56 13 30.8	15.10			
J115553.6+732416......	11 55 54.2	+73 23 44.7	15.00	15.65		

TABLE 2—*Continued*

Name (1RXS)	R.A. (J2000.0)	Decl. (J2000.0)	R_{USNO}	V_{GSC}	z	Type
J115719.0+333645......	11 57 17.4	+33 36 39.9	15.10		0.213	Gal
J115746.9+412642......	11 57 46.1	+41 26 37.4	14.40			
J120333.4+022939......	12 03 32.9	+2 29 34.5	14.40	13.88	0.077	AGN
J120547.8+584828......	12 05 48.9	+58 48 30.0	15.20			
J120954.9+062806......	12 09 54.6	+6 28 13.3	14.40			
J121104.0+700536......	12 11 03.9	+70 05 31.3	14.00	14.59		
J121157.1+055800......	12 11 57.5	+5 58 00.9	14.10			
J121217.1+280356......	12 12 16.2	+28 04 07.4	15.40		0.167	AGN
J121417.7+140312......	12 14 17.7	+14 03 12.6	13.90	13.96	0.081	AGN
J121510.9+073205......	12 15 10.9	+7 32 03.8	15.40		0.136	BL
J121752.1+300705......	12 17 52.0	+30 06 59.9	14.40		0.237	BL
J122044.5+690533......	12 20 47.9	+69 05 37.7	15.00			Gal
J122144.4+751848......	12 21 44.0	+75 18 38.5	14.80	14.37	0.070	Gal
J122523.1+042128......	12 25 22.9	+4 21 18.6	14.10			
J122623.7+372657......	12 26 23.3	+37 27 01.3	15.40			
J122635.9+455933......	12 26 36.9	+45 59 40.4	15.10			
J122745.1+084147......	12 27 44.8	+8 41 49.8	13.60		0.084	AGN
J122859.5+272527......	12 29 00.3	+27 25 21.4	15.10			
J123132.5+641420......	12 31 31.3	+64 14 17.5	15.00		0.170	BL
J123154.6+323248......	12 31 55.1	+32 32 40.8	14.40			
J123235.8+060315......	12 32 35.8	+6 03 09.7	15.10			
J123325.8+093119......	12 33 25.8	+9 31 23.0	14.10		0.415	AGN
J123658.8+631111......	12 36 58.7	+63 11 12.9	15.20			Gal
J123942.4+342453......	12 39 42.5	+34 24 55.7	15.20			
J124129.4+372206......	12 41 29.4	+37 22 01.7	13.90		0.063	AGN
J124141.2+344032......	12 41 39.9	+34 40 17.6	14.60	14.96		
J124211.3+331703......	12 42 10.6	+33 17 02.2	14.10	14.98	0.044	AGN
J124306.2+421233......	12 43 07.1	+42 12 31.1	15.30			
J124306.5+353859......	12 43 04.2	+35 39 16.8	14.90	15.23		
J124324.2+271645......	12 43 24.7	+27 16 48.6	14.70			Gal
J124339.6+700517......	12 43 39.3	+70 05 29.9	14.70	15.68		
J124701.3+442325......	12 47 00.1	+44 23 13.7	15.30			
J124717.2+481240......	12 47 16.3	+48 12 39.6	15.30			
J124818.9+582031......	12 48 18.7	+58 20 28.8	14.50			BL
J125005.7+263118......	12 50 05.7	+26 31 07.3	15.20		2.043	AGN
J125422.6+793618......	12 54 23.1	+79 36 12.8	15.20			
J125801.0+470237......	12 57 59.4	+47 02 01.3	14.80			
J125830.1+652121......	12 58 27.8	+65 21 30.7	15.40			
J125851.4+235532......	12 58 51.4	+23 55 26.6	13.90		0.071	AGN
J130052.9+564101......	13 00 50.7	+56 40 51.1	15.40			
J130258.8+162423......	13 02 58.8	+16 24 27.7	14.90	15.09	0.067	AGN
J130425.4+333512......	13 04 27.2	+33 35 13.0	14.40		0.188	Gal
J130803.0+035124......	13 08 03.1	+3 51 14.1	15.10			
J130947.1+081949......	13 09 47.0	+8 19 48.9	14.80		0.155	AGN
J131218.0+351524......	13 12 17.7	+35 15 20.3	14.70		0.184	AGN
J131334.0+725914......	13 13 32.0	+72 59 10.9	15.20		0.112	AGN
J131349.6+365357......	13 13 49.0	+36 53 57.7	15.40			
J131414.6+412347......	13 14 18.3	+41 24 30.1	15.30			
J131432.5+122706......	13 14 32.7	+12 27 17.9	14.70			
J131451.5+421819......	13 14 51.5	+42 18 19.1	14.80			
J131555.1+212508......	13 15 55.1	+21 25 21.5	15.00			
J131750.4+601047......	13 17 50.3	+60 10 40.6	15.30			
J132025.1+690018......	13 20 24.6	+69 00 12.4	15.40		0.067	AGN
J132042.4+601526......	13 20 45.3	+60 15 16.2	14.00			
J132314.2+463132......	13 23 14.9	+46 31 21.8	15.00		0.143	AGN
J132400.2+573918......	13 24 00.8	+57 39 16.1	13.90		0.115	BL
J132434.9+475802......	13 24 35.5	+47 58 00.7	15.10			
J132602.2+601206......	13 26 02.3	+60 11 59.4	15.10			
J132632.2+792850......	13 26 32.3	+79 28 51.7	15.00			
J132847.3+503808......	13 28 48.5	+50 37 53.5	15.30			
J132908.3+295018......	13 29 08.8	+29 50 23.9	15.40		0.047	AGN
J132943.8+315338......	13 29 43.6	+31 53 36.3	14.60		0.090	AGN
J133434.3+575019......	13 34 35.3	+57 50 15.3	15.00			
J133439.6+171748......	13 34 37.3	+17 17 49.4	15.30			
J133608.2+755041......	13 36 09.8	+75 50 34.9	15.20	15.28		
J133718.8+242306......	13 37 18.7	+24 23 02.9	14.30	14.26	0.107	AGN

TABLE 2—*Continued*

Name (1RXS)	R.A. (J2000.0)	Decl. (J2000.0)	R_{USNO}	V_{GSC}	z	Type
J133826.6+321252......	13 38 26.9	+32 12 51.9	15.20			
J133908.5+115855......	13 39 08.5	+11 58 53.5	15.30			
J133938.5+183055......	13 39 37.8	+18 30 59.4	15.10			
J134021.4+274100......	13 40 21.9	+27 41 26.8	14.20	14.19		
J134210.9+564219......	13 42 10.1	+56 42 10.9	14.60		0.040	AGN
J134335.3+413839......	13 43 35.7	+41 38 24.3	14.70	14.60		
J134356.7+253845......	13 43 56.7	+25 38 46.9	14.10	15.09		
J134357.3+271252......	13 43 57.4	+27 12 40.9	15.40		0.077	AGN
J134453.1+000525......	13 44 52.9	+0 05 19.7	14.80	15.51		
J134607.5+293814......	13 46 08.1	+29 38 10.5	14.10		0.076	AGN
J135022.2+094007......	13 50 22.1	+9 40 10.7	14.00			
J135022.2+094007......	13 50 22.1	+9 40 10.7	14.00			
J135143.8+242420......	13 51 43.9	+24 24 21.5	14.90			
J135436.0+180523......	13 54 35.6	+18 05 17.2	15.30		0.152	AGN
J135553.3+383427......	13 55 53.5	+38 34 29.1	15.00		0.051	AGN
J135821.2+360356......	13 58 24.5	+36 03 47.7	15.00	15.36		
J140310.5+375810......	14 03 08.8	+37 58 27.6	15.20			
J140519.6+020008......	14 05 19.4	+2 00 05.2	14.80		0.000	Star
J140606.1+580045......	14 06 04.8	+58 00 41.3	15.30			
J140622.2+222350......	14 06 21.9	+22 23 46.7	15.10		0.098	AGN
J140924.1+261827......	14 09 23.9	+26 18 21.3	15.40		0.940	AGN
J141336.8+702954......	14 13 36.7	+70 29 50.4	14.30		0.107	AGN
J141342.6+433938......	14 13 43.7	+43 39 44.1	14.70		0.089	Gal
J141346.6+263246......	14 13 45.3	+26 33 03.1	15.00	14.85		
J141700.5+445556......	14 17 00.8	+44 56 06.0	14.70	15.17	0.114	AGN
J141756.8+254329......	14 17 56.7	+25 43 24.7	15.30		0.237	BL
J141758.8+360749......	14 17 58.0	+36 08 10.5	15.20			
J141901.9+280942......	14 19 01.9	+28 09 41.7	14.80			
J142058.6+262450......	14 20 56.1	+26 24 22.5	15.40	14.95		
J142107.1+253818......	14 21 07.6	+25 38 20.8	15.40		1.050	AGN
J142129.8+474719......	14 21 29.8	+47 47 24.7	14.30	14.62	0.072	AGN
J142313.4+505537......	14 23 14.3	+50 55 38.1	15.20		0.274	AGN
J142425.2+595254......	14 24 24.1	+59 53 00.7	15.10	14.18		
J142630.6+390348......	14 26 30.7	+39 03 43.5	13.50			
J142700.5+234803......	14 27 00.4	+23 48 00.1	14.80			BL
J142725.3+194954......	14 27 25.0	+19 49 52.3	14.00	15.60	0.131	AGN
J142906.7+011708......	14 29 06.5	+1 17 05.0	13.60	13.21	0.086	AGN
J142924.3+451826......	14 29 25.0	+45 18 31.6	15.10			
J143308.8+232650......	14 33 08.4	+23 26 31.1	15.10			
J143445.8+332814......	14 34 45.3	+33 28 19.8	14.70			
J144034.4+242255......	14 40 34.3	+24 22 50.4	15.30			
J144248.5+120042......	14 42 48.2	+12 00 40.4	14.60		0.162	BL
J144645.8+403510......	14 46 45.9	+40 35 05.8	15.10		0.267	AGN
J144754.0+283323......	14 47 54.2	+28 33 23.7	15.40			
J144825.6+355955......	14 48 25.0	+35 59 46.4	15.00		0.111	AGN
J145307.6+255438......	14 53 08.0	+25 54 32.8	15.40			
J145307.8+215333......	14 53 08.3	+21 53 38.5	15.10			
J145559.0+492158......	14 55 59.5	+49 21 52.3	15.40			
J145729.4+083356......	14 57 29.0	+8 34 22.6	15.00		0.167	AGN
J145843.1+213614......	14 58 42.7	+21 36 10.0	15.30		0.062	AGN
J150023.0+763644......	15 00 22.3	+76 36 37.7	14.70	15.14		
J150124.1+302638......	15 01 24.2	+30 26 33.2	15.30			
J150317.5+681011......	15 03 16.3	+68 10 05.7	15.00			
J150332.0+295026......	15 03 32.1	+29 50 23.9	14.80			
J150506.8+435002......	15 05 07.3	+43 50 05.1	15.00			
J150752.3+515116......	15 07 52.6	+51 51 11.1	15.40			
J151040.8+333515......	15 10 41.1	+33 35 05.4	15.30			
J151105.3+525128......	15 11 06.0	+52 51 26.8	15.00			
J151447.0+351348......	15 14 46.9	+35 13 48.6	14.80			
J151634.5+205847......	15 16 34.5	+20 58 37.4	14.90			
J151845.3+061340......	15 18 45.7	+6 13 55.8	14.40		0.102	AGN
J151921.7+590823......	15 19 21.6	+59 08 23.6	14.40	15.09	0.078	AGN
J152558.6+181423......	15 25 58.5	+18 14 15.6	15.00			
J152806.5+132337......	15 28 06.9	+13 23 50.3	15.20			
J152912.9+381226......	15 29 14.0	+38 13 06.0	15.00	15.06	0.000	Star
J153140.9+201927......	15 31 41.3	+20 19 30.1	15.30			

TABLE 2—*Continued*

Name (1RXS)	R.A. (J2000.0)	Decl. (J2000.0)	R_{USNO}	V_{GSC}	z	Type
J153202.3+301631......	15 32 02.2	+30 16 28.6	13.50	15.30	0.064	BL
J153718.8+084355......	15 37 20.5	+8 44 08.7	15.20			
J153935.2+473545......	15 39 34.9	+47 35 53.1	15.00	14.87		
J154236.8+581153......	15 42 36.9	+58 11 45.0	13.90	14.07		
J154508.1+170935......	15 45 07.5	+17 09 50.4	14.70		0.045	AGN
J154732.3+102446......	15 47 32.2	+10 24 51.2	15.40			
J154751.7+025538......	15 47 51.9	+2 55 50.8	14.70		0.098	AGN
J154814.6+450040......	15 48 14.7	+45 00 27.8	14.90			
J155023.8+281125......	15 50 24.0	+28 11 17.2	15.20			
J155041.6+413915......	15 50 39.0	+41 39 29.9	15.30			
J155411.8+241415......	15 54 10.9	+24 14 40.5	15.40			
J155444.6+082202......	15 54 44.6	+8 22 21.6	15.40		0.119	AGN
J155543.2+111114......	15 55 43.0	+11 11 24.1	14.30	13.81	0.360	BL
J155643.0+294838......	15 56 42.8	+29 48 47.5	13.90	14.63	0.087	AGN
J155745.0+353020......	15 57 42.3	+35 30 29.9	13.90			
J155818.7+255118......	15 58 18.8	+25 51 24.4	15.30		0.070	AGN
J160529.2+720852......	16 05 26.0	+72 08 36.3	15.20			
J160740.7+254106......	16 07 40.2	+25 41 12.6	13.80	13.87		
J161047.7+330329......	16 10 47.8	+33 03 37.7	14.10		0.097	AGN
J161413.0+260412......	16 14 13.2	+26 04 15.9	15.10		0.131	AGN
J161601.3+323222......	16 16 01.8	+32 32 28.8	15.10		0.118	AGN
J161711.4+063816......	16 17 10.5	+6 38 43.0	15.20		0.092	AGN
J161804.5+672409......	16 18 03.8	+67 23 50.0	15.00			
J161809.2+361951......	16 18 09.4	+36 19 57.8	13.80		0.034	AGN
J161814.2+293828......	16 18 14.0	+29 38 08.9	15.30			
J162011.5+172413......	16 20 11.3	+17 24 27.5	15.20		0.114	AGN
J162100.4+254547......	16 21 00.3	+25 46 03.3	14.70			
J162114.3+181936......	16 21 14.4	+18 19 49.9	15.20		0.125	AGN
J162348.2+402948......	16 23 48.2	+40 29 59.0	15.00			
J162355.9+370018......	16 23 56.4	+37 00 44.9	15.30			
J162456.7+755457......	16 24 56.5	+75 54 55.8	13.70		0.200	AGN
J162607.6+335902......	16 26 07.2	+33 59 15.0	14.80		0.204	AGN
J163116.3+095545......	16 31 16.0	+9 55 57.9	15.00		0.092	AGN
J163323.3+471848......	16 33 23.5	+47 19 00.1	14.60		0.116	AGN
J163338.4+371311......	16 33 38.7	+37 13 14.8	14.70			
J163509.5+343956......	16 35 09.2	+34 40 03.4	15.40			
J163523.2+545304......	16 35 23.2	+54 53 00.3	15.00			
J164443.2+261909......	16 44 44.1	+26 19 04.6	15.20			
J164550.2+792129......	16 45 49.5	+79 21 28.6	14.90			
J164625.8+392922......	16 46 26.0	+39 29 32.2	14.60		0.100	AGN
J164735.4+495001......	16 47 34.8	+49 49 59.8	14.60		0.047	AGN
J164801.1+295650......	16 48 00.8	+29 56 57.4	14.30		0.101	AGN
J165141.2+721824......	16 51 39.6	+72 18 42.7	15.40			
J165253.7+400927......	16 52 56.6	+40 08 43.1	15.00			
J170328.3+614114......	17 03 28.9	+61 41 10.1	14.70			
J170425.2+333145......	17 04 22.4	+33 31 40.3	14.90	13.46		
J170535.1+334011......	17 05 34.9	+33 40 12.3	14.90			
J171013.2+334410......	17 10 13.5	+33 44 03.6	14.80		0.208	AGN
J171322.8+325631......	17 13 22.6	+32 56 28.8	14.50		0.100	AGN
J171410.8+575826......	17 14 11.5	+57 58 33.5	14.90		0.092	AGN
J171601.3+311215......	17 16 01.9	+31 12 13.5	14.40	15.48	0.111	AGN
J171935.9+424518......	17 19 33.9	+42 45 22.5	15.00			
J172320.5+341756......	17 23 20.8	+34 17 57.8	14.50		0.206	AGN
J172609.3+743103......	17 26 08.3	+74 31 03.4	14.60		0.052	AGN
J172855.8+515654......	17 28 54.6	+51 56 49.2	14.90	14.21		
J173114.5+323250......	17 31 15.2	+32 32 58.4	13.90	14.05		
J174025.8+514942......	17 40 25.7	+51 49 42.4	14.50			
J174815.0+582333......	17 48 15.3	+58 23 35.5	15.00			
J174839.6+530240......	17 48 37.6	+53 02 45.4	15.40			
J214923.8+092921......	21 49 23.7	+9 28 47.3	15.30			
J215912.7+095247......	21 59 12.3	+9 52 43.4	14.90		0.101	AGN
J222602.8+172245......	22 26 02.2	+17 22 47.0	15.40			
J224939.6+110016......	22 49 39.6	+11 00 29.2	14.80		0.084	AGN
J225207.7+145448......	22 52 08.1	+14 54 49.6	14.80		0.130	AGN
J225636.8+052522......	22 56 36.5	+5 25 17.2	14.90		0.066	AGN
J225932.9+245505......	22 59 32.9	+24 55 05.6	13.50	15.07	0.034	AGN

TABLE 2—*Continued*

Name (1RXS)	R.A. (J2000.0)	Decl. (J2000.0)	R_{USNO}	V_{GSC}	z	Type
J231357.3+144424......	23 13 56.3	+14 43 53.5	14.90			
J231517.5+182825......	23 15 17.1	+18 28 14.4	15.00		0.104	AGN
J232339.1+090842......	23 23 39.0	+9 08 50.6	14.80		0.068	AGN
J233606.6+241555......	23 36 06.1	+24 15 58.3	14.50		0.039	AGN
J233641.8+235526......	23 36 42.2	+23 55 29.0	14.20		0.127	Gal
J233739.8+001604......	23 37 40.7	+0 16 35.3	14.90			
J234031.5+102934......	23 40 31.0	+10 29 39.0	14.70			
J234339.0+024445......	23 43 39.8	+2 45 03.9	15.40		0.091	AGN
J235257.1+032008......	23 52 58.0	+3 20 17.3	14.30		0.086	AGN
J235754.3+132418......	23 57 53.8	+13 24 09.6	15.30			

NOTE.—Units of right ascension are hours, minutes, and seconds, and units of declination are degrees, arcminutes, and arcseconds.

1. $-0.9 \leq \mathrm{HR1} \leq 0.9$, where HR1, the hardness ratio 1, is defined as $(A - B)/(A + B)$, with the *ROSAT* PSPC count rates A in the hard band ($0.5 \div 2.0$ keV) and B in the soft band ($0.1 \div 0.4$ keV);
2. $-0.6 \leq \mathrm{HR2} \leq +0.8$, where HR2, the hardness ratio 2, is defined as $(C - D)/(C + D)$, with the *ROSAT* PSPC count rates C in the hard band ($0.9 \div 2.0$ keV) and D in the soft band ($0.5 \div 0.9$ keV).

4. SPECTROSCOPIC FOLLOW-UP

In the following, we concentrate our discussion on the sample of northern objects for which the follow-up spectroscopy is more advanced. The southern sample will be described elsewhere. The list of the quasar candidates and the results of the spectroscopy are listed in Tables 2 and 3. It should be noted that Tables 2 and 3 cannot be considered a list of optical identifications of X-ray sources. The cross-correlation procedure defined in the previous section aims at finding optical objects in a desired magnitude range around X-ray sources. In some cases an entry in Table 2 or 3 may exist even if the true identification of the X-ray source is another (typically fainter) optical object. For example, even if the optical counterpart of the RASS source J013624.3+205712 is known to be the QSO 3C47.0, with $V \simeq 18.1$ and $z = 0.425$, in the tables we list an object with $R_{USNO} = 14.7$ that happens to fulfill the criteria of the cross-correlation.

The follow-up observations of the QSO candidates have been carried out at the 1.8 m telescope in Asiago with a Boller and Chivens spectrograph or with the Asiago Faint Object Spectrograph and Camera (AFOSC), at the 1.5 m ESO, 1.5 m Danish, and NTT telescopes in La Silla with a Boller and Chivens spectrograph, DFOSC, and EMMI, respectively, and with the 90 inch (2.3 m) telescope at Kitt Peak. The resolution of the spectra ranges between 10 and 30 Å.

The reduction process used the standard MIDAS facilities (Banse et al. 1988) available at the Padua Department of Astronomy and at ESO in Garching. The raw data were sky-subtracted and corrected for pixel-to-pixel sensitivity variations by division with a suitably normalized exposure of the spectrum of an incandescent source (flat field). Wavelength calibration was carried out by comparison with exposures of HeAr, He, Ar, and Ne lamps. Relative flux calibration was carried out by observations of spectrophotometric standard stars (Oke 1990).

The identification classes in Tables 2, 3, and 4 are the following: "AGN" indicates emission-line object, irrespective of the line width; "Star" indicates star; "Gal" indicates galaxy; and "BL" indicates BL Lac object. Identifications as "BL Lac" or "Gal" have been taken from the NASA/IPAC Extragalactic Database. Uncertain identifications and redshifts are indicated with a colon. To test the reliability of our selection, additional candidates, selected with less restrictive criteria than those reported in the previous section, were observed. They are reported in Table 4. The spectra of the AGNs found during the follow-up spectroscopy are shown in Figure 2.

5. FIRST RESULTS

The spectroscopic observations of the northern sample are still incomplete: only 45% of the candidates have been identified. Different areas of the sky, in particular different strips in right ascension, have been observed down to different magnitude limits. Tables 5 and 6 list the extension of the area covered with a complete spectroscopic follow-up as a function of the limiting magnitude. In the following computations we have adopted for the northern sample the effective areas listed in Tables 5 and 6, which take into account

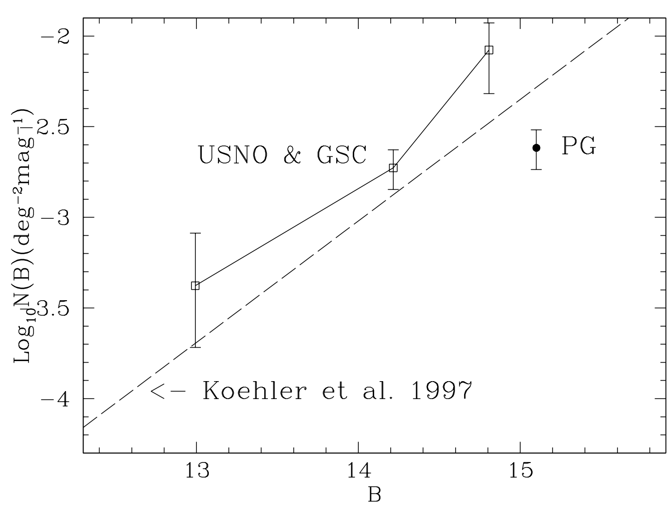

FIG. 3.—The log N-log S relation of QSOs. Squares represent the present sample and are QSOs with $z \geq 0.04$. A correction of -0.037 to the values of the last in Table 7 has been applied to account for the Bennet bias. The dashed line is the relation found by Köhler et al. (1997) for QSOs with $0.07 \leq z \leq 2.2$. The circle is the point derived from the PG survey.

TABLE 3

GSC SAMPLE

Name (1RXS)	R.A.	Decl.	V_{GSC}	z	Type
J000350.4+020340......	00 03 49.7	+2 03 58.9	13.28		
J001219.0+100602......	00 12 19.3	+10 06 45.8	14.02		
J003633.7+254513......	00 36 32.4	+25 45 18.2	14.32		
J004400.0+313729......	00 44 00.0	+31 37 04.3	14.42		
J004719.4+144215......	00 47 19.4	+14 42 11.8	14.00	0.039	AGN
J004931.6+112832......	00 49 32.0	+11 28 26.0	14.37	0.275	AGN
J005017.9+083734......	00 50 17.4	+8 37 35.3	14.31		
J005029.2+112902......	00 50 27.9	+11 29 10.9	14.37	0.000	Star
J005351.3+221222......	00 53 50.9	+22 12 13.7	14.38		
J005953.3+314934......	00 59 53.3	+31 49 37.4	13.74	0.015	AGN
J010014.0+055200......	01 00 14.1	+5 51 54.8	14.00		
J011125.4+152625......	01 11 24.8	+15 26 26.8	13.59		
J011704.2+000025......	01 17 03.6	+0 00 27.0	14.50	0.040	AGN
J012732.9+191043......	01 27 32.5	+19 10 43.8	11.80	0.017	AGN
J015240.2+014718......	01 52 39.6	+1 47 16.8	13.92	0.080	BL
J015242.1+010040......	01 52 41.9	+1 00 25.1	13.57	0.230	Gal
J020026.7+024012......	02 00 26.3	+2 40 09.9	12.77	0.078	AGN
J024920.8+191813......	02 49 20.7	+19 18 14.2	14.18	0.031	AGN
J025153.2+222735......	02 51 53.7	+22 27 35.7	12.40	0.000	Star
J075704.9+583245......	07 57 06.2	+58 32 58.7	14.48	0.000	Star
J080525.8+753424......	08 05 23.7	+75 34 34.7	14.40		
J081228.3+623627......	08 12 28.2	+62 36 23.3	14.15		
J081517.8+460429......	08 15 16.9	+46 04 30.7	14.24		
J081917.9+642943......	08 19 17.6	+64 29 40.0	14.40	0.039	AGN
J082407.3+613612......	08 24 11.3	+61 36 11.3	14.01		
J083137.6+192339......	08 31 38.3	+19 23 45.2	11.43		
J083811.0+245336......	08 38 10.9	+24 53 42.4	12.80		
J084456.2+425826......	08 44 56.6	+42 58 35.1	14.40		
J084602.9+830757......	08 46 17.9	+83 07 43.5	14.47		
J084742.5+344506......	08 47 42.5	+34 45 03.8	13.64	0.064	AGN
J090008.1+743419......	09 00 03.7	+74 34 26.4	14.37		
J091230.8+155531......	09 12 31.0	+15 55 24.3	13.42		
J091552.3+090056......	09 15 51.8	+9 00 50.9	12.99	0.000	Star
J091826.2+161825......	09 18 26.0	+16 18 19.2	13.21	0.030	AGN
J092030.8+013544......	09 20 31.1	+1 35 37.1	14.14		
J092108.2+480201......	09 21 11.3	+48 01 59.2	13.84		
J092343.0+225437......	09 23 43.0	+22 54 32.7	13.43		
J092512.3+521716......	09 25 13.0	+52 17 11.4	13.66	0.036	AGN
J092603.6+124406......	09 26 03.3	+12 44 03.3	13.71	0.028	AGN
J092702.8+390221......	09 27 04.0	+39 02 17.8	13.59		
J092705.7+374157......	09 27 03.0	+37 42 05.5	14.12		
J093701.0+010548......	09 37 01.0	+1 05 43.0	13.87	0.051	AGN
J093900.4+253008......	09 39 00.4	+25 30 14.6	14.41		
J094204.0+234106......	09 42 04.8	+23 41 06.5	14.15	0.021	Gal
J094432.8+573544......	09 44 04.7	+57 33 28.1	14.13		
J094851.0+153901......	09 48 50.2	+15 38 34.6	14.25		
J095340.4+014154......	09 53 41.3	+1 42 01.7	13.98		
J095624.5+064803......	09 56 23.8	+6 48 01.6	14.34		
J095919.3+435033......	09 59 19.2	+43 50 35.4	13.57		
J100446.0+144651......	10 04 47.6	+14 46 45.2	14.23	0.082	AGN
J100641.5+213955......	10 06 43.6	+21 39 27.7	14.50		
J101218.6+631133......	10 12 21.6	+63 11 32.1	14.21		
J101718.0+291439......	10 17 18.3	+29 14 33.8	13.96	0.048	AGN
J101912.1+635802......	10 19 12.6	+63 58 02.2	13.69	0.041	AGN
J102334.6+443346......	10 23 35.0	+44 33 41.5	13.86		
J102407.0+273130......	10 24 06.7	+27 31 22.7	14.22		
J102611.1+523755......	10 26 06.2	+52 37 56.3	13.99		
J104038.7+373233......	10 40 39.0	+37 32 31.3	13.36		
J104333.4+010109......	10 43 32.8	+1 01 08.6	13.99	0.072	AGN
J104439.4+384541......	10 44 39.1	+38 45 34.8	14.48	0.036	Gal
J105121.3+360728......	10 51 21.3	+36 07 27.4	13.31		
J105214.2+055514......	10 52 15.3	+5 55 08.2	13.96		
J105328.5+053052......	10 53 29.7	+5 30 30.2	13.92		
J105340.7+525310......	10 53 41.2	+52 53 01.7	14.25		
J110159.1+572316......	11 02 00.1	+57 22 50.3	14.43		
J110310.2+363911......	11 03 10.7	+36 39 06.3	13.41		

TABLE 3—*Continued*

Name (1RXS)	R.A.	Decl.	V_{GSC}	z	Type
J110321.2+133759......	11 03 21.8	+13 37 52.4	12.90		
J110455.7+433421......	11 04 56.0	+43 34 03.0	14.29		
J110943.6+214519......	11 09 41.1	+21 44 24.2	14.33	0.032	Gal
J111300.1+102518......	11 13 00.2	+10 25 12.3	14.29		
J111349.5+093518......	11 13 49.7	+9 35 10.9	12.42	0.029	AGN
J112147.3+114420......	11 21 47.1	+11 44 18.2	14.48	0.050	AGN
J112150.8+405147......	11 21 51.2	+40 51 46.4	13.97		
J112315.6+193610......	11 23 14.6	+19 35 25.5	14.13		
J112536.7+542243......	11 25 36.1	+54 22 56.9	14.33	0.021	AGN
J114116.2+215624......	11 41 16.2	+21 56 21.1	13.25	0.063	AGN
J114516.1+794054......	11 45 16.1	+79 40 52.6	13.50	0.065	AGN
J114738.0+050119......	11 47 37.4	+5 01 09.3	12.09		
J114741.4+001524......	11 47 41.7	+0 15 24.1	14.23		
J115658.6+241523......	11 56 55.8	+24 15 35.2	13.55	0.142	Gal
J120333.4+022939......	12 03 32.9	+2 29 34.5	13.88	0.077	AGN
J120829.9+132752......	12 08 29.8	+13 28 06.0	13.31		
J121417.7+140312......	12 14 17.7	+14 03 12.6	13.96	0.081	AGN
J121607.4+504926......	12 16 07.0	+50 49 30.2	14.25	0.031	AGN
J121900.7+110727......	12 18 59.8	+11 07 53.9	13.53		
J121920.9+063838......	12 19 21.5	+6 38 43.9	13.22		
J122005.9+650552......	12 20 10.3	+65 05 55.2	14.34		
J122144.4+751848......	12 21 44.0	+75 18 38.5	14.37	0.070	AGN
J122147.1+015637......	12 21 46.6	+1 56 35.3	13.76		
J122306.6+103722......	12 23 06.7	+10 37 16.8	12.25	0.026	Gal
J122324.4+024040......	12 23 24.2	+2 40 44.9	12.81	0.023	AGN
J122512.5+321354......	12 25 13.1	+32 14 00.9	14.38	0.061	AGN
J122906.5+020311......	12 29 06.7	+2 03 08.1	12.26	0.158	AGN
J123014.2+251805......	12 30 14.2	+25 18 05.9	14.49	0.135	BL
J123055.5+315207......	12 30 55.8	+31 52 16.1	14.19		
J123203.6+200930......	12 32 03.6	+20 09 29.6	12.87	0.064	AGN
J123415.2+481306......	12 34 16.0	+48 13 06.9	14.31		
J123651.1+453907......	12 36 51.2	+45 39 04.4	13.59	0.029	AGN
J123658.6+455341......	12 36 57.0	+45 53 26.0	14.41		
J124147.5+564506......	12 41 46.7	+56 45 13.5	13.13		
J124312.5+362743......	12 43 12.7	+36 27 43.8	11.42		
J124955.0+102312......	12 49 54.5	+10 23 08.3	14.03		
J125731.7+354313......	12 57 32.7	+35 43 19.9	14.19		
J130934.9+285908......	13 09 36.1	+28 59 15.0	13.95		
J131957.2+523533......	13 19 58.8	+52 35 27.7	13.49		
J132016.3+330828......	13 20 14.7	+33 08 36.1	13.17	0.036	Gal
J133451.1+374616......	13 34 51.9	+37 46 20.7	13.83		
J133718.8+242306......	13 37 18.7	+24 23 02.9	14.26	0.107	AGN
J133752.7+204634......	13 37 50.9	+20 46 39.8	14.20		
J134021.4+274100......	13 40 21.9	+27 41 26.8	14.19		
J134952.7+020446......	13 49 52.8	+2 04 44.3	13.32		
J135119.8+033722......	13 51 20.2	+3 37 16.4	13.77		
J135304.8+691832......	13 53 03.4	+69 18 29.5	12.92		
J135420.2+325547......	13 54 20.0	+32 55 47.9	12.78	0.026	AGN
J140226.8+054103......	14 02 26.3	+5 40 51.8	13.26		
J141722.1+452544......	14 17 21.9	+45 25 46.7	13.94		
J141759.6+250817......	14 17 59.2	+25 08 13.2	11.02		
J141802.6+800710......	14 17 59.3	+80 07 02.2	14.19		
J142425.2+595254......	14 24 24.1	+59 53 00.7	14.18		
J142906.7+011708......	14 29 06.5	+1 17 05.0	13.21	0.086	AGN
J143104.8+281716......	14 31 04.8	+28 17 14.8	13.43	0.046	AGN
J143452.3+483938......	14 34 52.4	+48 39 42.6	13.38		
J143729.6+412842......	14 37 29.9	+41 28 35.2	13.70		
J144713.2+570205......	14 47 13.0	+57 01 56.7	13.97		
J150401.5+102620......	15 04 01.2	+10 26 16.2	14.19	0.036	AGN
J150406.7+485856......	15 04 07.1	+48 58 55.1	14.05		
J150724.6+433356......	15 07 23.5	+43 33 51.6	13.64		
J150950.2+415540......	15 09 49.7	+41 55 38.8	14.29		
J151750.8+050615......	15 17 51.7	+5 06 27.4	13.98	0.039	AGN
J151837.9+404506......	15 18 38.9	+40 45 00.0	14.19		
J153345.9+690037......	15 33 44.7	+69 00 34.0	13.73		
J153412.6+625902......	15 34 13.2	+62 58 57.7	13.76		
J153522.9+600515......	15 35 24.5	+60 05 15.3	13.17		

TABLE 3—*Continued*

Name (1RXS)	R.A.	Decl.	V_{GSC}	z	Type
J153552.0+575404......	15 35 52.4	+57 54 08.5	13.91	0.030	AGN
J153704.2+374830......	15 37 04.0	+37 48 26.9	13.43		
J153944.2+275113......	15 39 43.9	+27 50 58.1	13.74		
J154236.8+581153......	15 42 36.9	+58 11 45.0	14.07		
J154348.9+401343......	15 43 50.5	+40 13 41.6	13.05		
J154532.3+420500......	15 45 34.7	+42 05 07.2	13.87		
J155305.9+445749......	15 53 05.1	+44 57 39.9	14.16		
J155532.2+351207......	15 55 32.7	+35 11 54.8	13.41		
J155543.2+111114......	15 55 43.0	+11 11 24.1	13.81	0.360	BL
J155625.4+090311......	15 56 26.0	+9 03 19.2	14.47	0.042	AGN
J155703.2+635029......	15 57 03.3	+63 50 27.4	14.01	0.030	AGN
J155721.3+445902......	15 57 22.6	+44 58 54.3	14.16		
J155909.5+350144......	15 59 09.7	+35 01 47.3	14.14	0.031	AGN
J160740.7+254106......	16 07 40.2	+25 41 12.6	13.87		
J161004.4+671030......	16 10 04.0	+67 10 25.9	13.67	0.067	BL
J161124.8+585106......	16 11 24.6	+58 51 01.3	14.24	0.032	AGN
J161301.5+371656......	16 13 01.7	+37 17 15.2	14.37	0.070	AGN
J161801.9+775230......	16 17 59.8	+77 52 34.5	13.55		
J161951.7+405834......	16 19 51.3	+40 58 47.5	14.31		
J162013.1+400858......	16 20 12.7	+40 09 05.7	14.18		
J162409.7+260421......	16 24 09.3	+26 04 31.4	14.03	0.040	AGN
J162552.9+434654......	16 25 53.3	+43 46 51.9	13.70		
J162903.6+361911......	16 29 05.3	+36 18 58.7	14.45	0.000	Star
J163056.3+361848......	16 30 56.1	+36 18 48.5	14.45		
J165057.5+222653......	16 50 57.8	+22 26 47.8	14.29		
J165352.6+394538......	16 53 52.2	+39 45 36.3	11.27	0.033	BL
J165551.7+214559......	16 55 51.4	+21 46 01.2	13.79		
J171227.2+355256......	17 12 28.5	+35 53 02.1	13.73	0.027	AGN
J171959.4+241202......	17 19 59.7	+24 12 07.6	14.08		
J172855.8+515654......	17 28 54.6	+51 56 49.2	14.21		
J173114.5+323250......	17 31 15.2	+32 32 58.4	14.05		
J174700.3+683626......	17 46 59.8	+68 36 36.1	13.78	0.063	Gal
J174702.0+493803......	17 47 03.0	+49 38 19.3	14.20		
J213740.3+013711......	21 37 39.9	+1 37 16.4	13.35		
J222408.1+172903......	22 24 08.1	+17 28 47.4	14.42		
J225314.2+040957......	22 53 11.9	+4 10 36.1	14.35		
J225453.7+241449......	22 54 55.1	+24 14 45.5	14.18		
J230315.7+085226......	23 03 15.6	+8 52 26.9	11.05	0.016	AGN
J230706.6+163153......	23 07 05.3	+16 32 27.1	13.78		
J231341.0+140113......	23 13 40.5	+14 01 15.6	13.86	0.041	AGN
J233413.9+073637......	23 34 13.9	+7 37 01.2	13.86		
J234106.5+093805......	23 41 06.6	+9 38 09.1	14.38		
J234728.8+242743......	23 47 28.8	+24 27 45.8	13.65		
J234953.5+242754......	23 49 53.3	+24 27 51.6	13.65		
J235122.7+234417......	23 51 21.5	+23 44 24.4	14.02		

the incompleteness factors estimated in the previous sections.

5.1. *Quasar Counts*

Figure 3 shows the log N-log S relation of QSOs brighter than $M_B = -23$ mag with $z \geq 0.04$, for the USNO and GSC subsamples together.[5] The log N-log S relation has been computed with the $\sum 1/\text{Area}_{\max}$ method, a convenient approach when the various subareas have very different magnitude limits. Table 7 lists the differential QSO counts.

The log N-log S relation found in the present survey is consistent with a single power-law distribution with slope 0.67 reported by Köhler et al. (1997) for QSOs with $0.07 \leq z \leq 2.2$ with a slightly higher normalization: if we fix $\beta = 0.67$ in a $\log N = \beta B + k$ relation, we find $k = -12.15^{+0.17}_{-0.19}$. If we restrict our sample to $z > 0.07$, we find $k = -12.2 \pm 0.2$, in agreement with the normalization, $k = -12.4$, of Köhler et al. (1997).

A comparison with the BQS (Schmidt & Green 1983) shows that at $B \sim 15.5$ the cumulative BQS counts are about a factor of 3 lower. This confirms previous findings by Goldschmidt et al. (1992), LC97, and Köhler et al. (1997).

5.2. *QSO Luminosity Function at* $0.04 < z \leq 0.3$

A preliminary analysis of the QSO optical LF has been carried out on the basis of the present sample. A more detailed discussion of the complete spectroscopic database will be developed elsewhere (Omizzolo et al. 2000). To compute the LF at $0.04 < z \leq 0.3$, we have used the generalized $1/V_{\max}$ "coherent" estimator (Avni & Bahcall 1980)

[5] In the present paper, the k-corrections are computed on the basis of the composite spectrum of Cristiani & Vio (1990), and galactic extinction is taken into account according to Burstein & Heiles (1982). The values $q_0 = 0.5$ and $H_0 = 50$ km s^{-1} Mpc^{-1} are adopted throughout.

TABLE 4

OTHER SPECTROSCOPIC IDENTIFICATIONS

Name (1RXS)	R.A.	Decl.	B_J	z	Type
J000011.9+052318......	00 00 11.80	+05 23 17.3	16.40	0.039	AGN
J000637.1+434223......	00 06 36.60	+43 42 28.3	14.80	0.166	AGN
J000805.6+145027......	00 08 05.70	+14 50 23.3	14.50	0.043	AGN
J001409.9+304928......	00 14 01.00	+30 49 24.3	18.20	:0.000	Star
J004649.4+152741......	00 46 50.00	+15 27 52.6	16.10	:0.078	AGN
J005050.6+353645......	00 50 50.80	+35 36 42.2	14.60	0.056	AGN
J005346.9+223209......	00 53 46.20	+22 32 22.5	15.80	0.148	AGN
J011205.2+224452......	01 12 05.80	+22 44 38.6	15.80	0.000	Star
J020012.5+130317......	02 00 13.90	+13 03 13.1	16.20	0.000	Star
J130710.9+394540......	13 07 11.50	+39 45 33.1	15.40	0.076	AGN
J144240.3+262330......	14 42 40.80	+26 23 32.4	16.40	:0.110	AGN
J151601.5+020055......	15 16 01.40	+2 00 59.8	16.80	0.105	AGN
J170320.4+373731......	17 03 20.10	+37 37 23.8	16.20	...	AGN
J171235.5+245037......	17 12 35.80	+24 50 26.8	17.50	...	AGN
J221832.8+192527......	22 18 31.30	+19 25 42.8	14.40	0.000	Star
J232841.4+224853......	23 28 42.90	+22 49 43.7	15.20	0.000	Star
J234114.9+142820......	23 41 15.90	+14 28 43.7	16.80	0.000	Star
J235959.1+083355......	23 59 59.30	+8 33 54.1	15.40	0.083	AGN

in a slightly modified version that tries to estimate in an unbiased manner the volume-luminosity space "available" to each object (see the method of Page & Carrera 1999) and takes into account the evolution of the LF within the redshift interval. Errors were estimated from Poisson statistics (Gehrels 1986). The data values of the LF at $0.04 < z \leq 0.3$ are listed in Table 8.

Figures 4*a* and 4*b* show the comparison of the newly derived QSO LF at $0.04 < z \leq 0.3$ with data at higher redshift, up to $z = 2.2$ (LC97), and with a PLE and an LDLE parameterization, respectively. The points in the range $0.04 < z \leq 0.3$ are the result of the present survey; the data in the other redshift ranges are derived from LC97. No effort has been made in the derivation of the LF at $0.04 < z \leq 0.3$ to subtract the luminosity of the host galaxy.

The PLE parameterization is the global best fit to the QSO LF derived in the interval $0.3 < z < 2.2$ by LC97 (model B), who found it to be inconsistent with the data at $0.3 < z < 0.6$ at a 3 σ level. The present result confirms and strengthens the conclusion of LC97 that if we compare the prediction of the model B PLE of LC97 in the range $0.04 < z \leq 0.3$, the value $\chi^2 \simeq 14$ for the five data points of Table 8 is derived, corresponding to a formal probability of 1.9%.

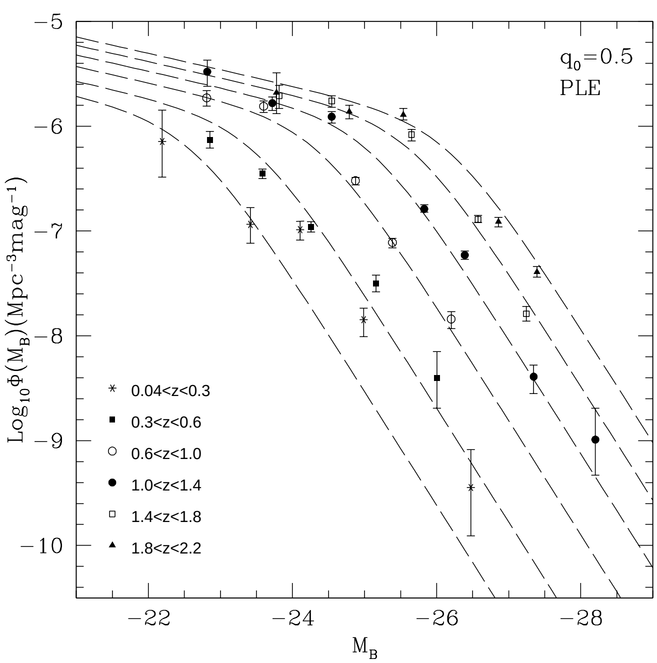

FIG. 4*a*

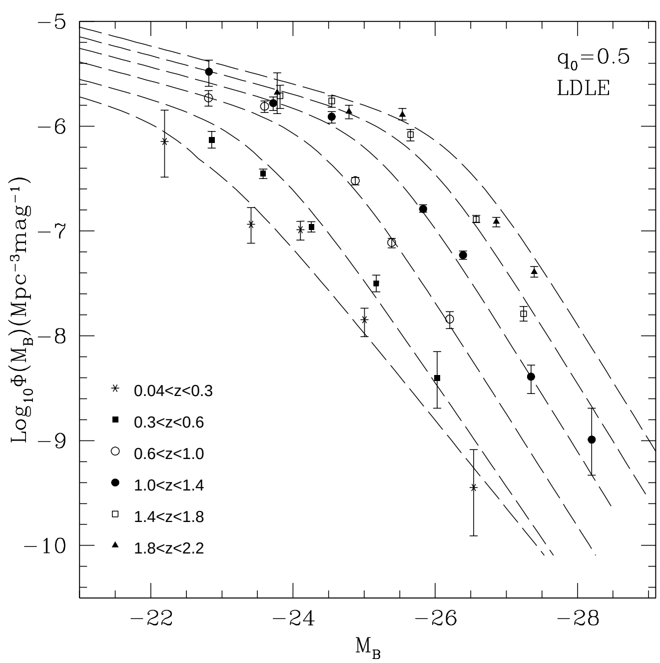

FIG. 4*b*

FIG. 4.—Luminosity function of QSOs compared with (*a*) a parameterization of pure luminosity evolution (see text) and (*b*) a parameterization of luminosity dependent luminosity evolution. The points in the range $0.04 < z \leq 0.3$ are the result of the present survey; the remaining data are derived from LC97.

TABLE 5

USNO SPECTROSCOPIC FOLLOW-UP ($0 < \delta < 90$)

R_{min}	R_{max}	AR_{min}	AR_{max}	Area
13.50......	15.40	00.00	01.00	315.250
13.50......	14.55	01.00	06.00	662.000
13.50......	15.40	06.00	08.00	32.750
13.50......	14.40	08.00	09.00	366.750
13.50......	14.40	09.00	10.00	732.750
13.50......	13.90	10.00	11.00	688.000
13.50......	14.40	11.00	12.00	652.750
13.50......	13.90	12.00	13.00	727.566
13.50......	14.60	13.00	14.00	758.042
13.50......	14.60	14.00	15.00	781.193
13.50......	13.70	15.00	16.00	730.482
13.50......	14.60	16.00	17.00	780.750
13.50......	14.60	17.00	18.00	388.000
13.50......	14.90	18.00	22.00	93.500
13.50......	14.50	22.00	24.00	454.750

TABLE 6

GSC SPECTROSCOPIC FOLLOW-UP ($0 < \delta < 90$)

V_{min}	V_{max}	AR_{min}	AR_{max}	Area
11.00......	14.00	00.00	02.00	646.250
11.00......	14.50	02.00	04.00	298.000
11.00......	14.50	04.00	06.00	32.750
11.00......	13.50	06.00	08.00	32.750
13.20......	14.10	08.00	09.00	366.750
11.00......	13.75	09.00	10.00	732.750
13.96......	14.10	10.00	11.00	688.000
13.45......	13.75	11.00	12.00	652.750
11.85......	13.00	12.00	13.00	727.566
11.00......	13.35	13.00	14.00	758.042
11.00......	13.25	14.00	15.00	781.193
13.80......	14.05	15.00	16.00	730.482
11.00......	13.75	16.00	18.00	1168.750
11.00......	14.50	18.00	20.00	000.000
11.00......	14.50	20.00	22.00	935.000
11.00......	13.50	22.00	24.00	454.750

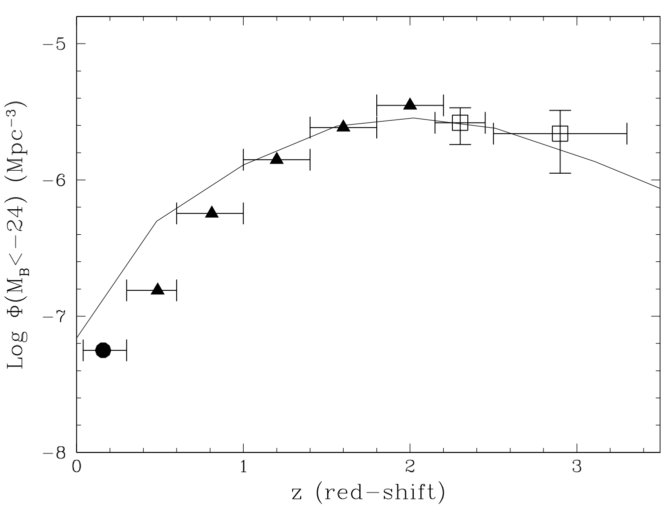

FIG. 5.—Continuous line representing evolution of the space density of quasars with $M_B < -24$ predicted by the ΛCDM model described in the text (KH). The circle represents data from the present work; squares, data from Hartwick & Schade (1990). Triangles are derived from LC97.

TABLE 7

DIFFERENTIAL QSO COUNTS

B Interval	$\langle B \rangle$	N	log (surf den) ($mag^{-1} deg^{-2}$)
12.5–13.5......	13.0	3	−3.34
13.5–14.5......	14.2	19	−2.69
14.5–15.5......	14.8	24	−2.04

Figure 4*b* shows that an LDLE parameterization of the type of model C of LC97 can reproduce the data in a much more satisfactory way. The best agreement with the data from $z = 0.04$ to $z = 2.2$ is obtained, assuming the functional form (LC97)

$$\Phi(M_B, z) = \frac{\Phi^*}{10^{0.4[M_B - M_B^*(z)](\alpha+1)} + 10^{0.4[M_B - M_B^*(z)](\beta+1)}} , \quad (3)$$

with

$$M_B^*(z) = M_B^*(z=2) - 2.5k \log [(1+z)/3] \quad (4)$$

and

$$\text{for } M_B \le M_B^*(z), k = k_1 + k_2[M_B - M_B^*(z)]e^{-z/.40} ,$$
$$\text{for } M_B > M_B^*(z), k = k_1 , \quad (5)$$

where α and β correspond to the faint-end and bright-end slopes of the optical LF, respectively, and $M_B^*(z=2)$ is the magnitude of the break in the double power-law shape of the LF at $z = 2$. The actual values adopted in the LDLE parameterization are $\Phi^* = 9.8 \times 10^{-7}$ mag^{-1} Mpc^{-3}, $M_B^*(z=2) = -26.3$, $k_1 = 3.33$, $k_2 = 0.37$, $\alpha = -1.45$, and $\beta = -3.76$, providing a χ^2 probability of $\simeq$58% in the range $0.04 < z \le 0.3$ when compared with the five data points of Table 8.

6. DISCUSSION

Franceschini et al. (1994) and La Franca et al. (1995) have shown that the QSO emission at the soft X-ray and visible wavelengths scales linearly. A confirmation of the constant ratio L_X/L_O and independence from both L_O and z comes from Yuan et al. (1998). Boyle et al. (1994) derived an XLF comparable with the QSO OLF known at that epoch with an evolutionary rate $L_X(z) = L_X(0)(1+z)^{3.25}$, similar to the optical one. These works favor a scenario in which essentially the same QSO population is observed, in both the soft X-ray and the optical bands. In this way, the flattening of the OLF observed in the present survey should be reflected in a flattening in the corresponding soft X-ray LF. Indeed, Miyaji, Hasinger, & Schmidt (1999) show that the bright part of the 0.5–2 keV LF flattens with decreasing redshift

TABLE 8

QSO LUMINOSITY FUNCTION AT $0.04 < z < 0.3$

M_B Interval	$\langle M_B \rangle$	N	log LF $Mpc^{-3} mag^{-1}$
−21.5 to −22.5......	−22.04	3	−6.05
−22.5 to −23.5......	−23.31	9	−6.84
−23.5 to −24.5......	−24.10	23	−6.89
−24.5 to −25.5......	−25.10	11	−7.75
−25.5 to −28.5......	−26.72	2	−9.35

from $1 + \beta \simeq 3.5$ at $0.4 < z < 0.8$ to $1 + \beta \simeq 2.6$ at $0.015 < z < 0.2$, which is similar to what we observe in the optical spectrum: $1 + \beta \simeq 3.7$ at $0.6 < z < 1.0$ and $1 + \beta \simeq 3.1$ at $0.04 < z \leq 0.3$.

The decline of the space density of quasars from a peak around redshift $z = 2$ to the present epoch has been modeled by several authors in the framework of hierarchical theories of structure formation (Cattaneo 1999; Haiman & Menou 1999; Kauffmann & Haehnelt 1999, hereafter KH; Monaco, Salucci, & Danese 1999). In particular, KH have attempted to reproduce quantitatively the evolution of the quasar number density incorporating a scheme for the growth of massive black holes (MBHs) into semianalytical models following the evolution of galaxies in CDM-dominated scenarios. Together with the decrease in the merging rates and in the amount of gas available to fuel the MBHs, which are built-in features of the semianalytic models, KH assume an increase of the timescale for gas accretion to reproduce the steep decline in the number density of quasars from $z \sim 2$ to $z = 0$. Other authors have followed similar recipes, assuming a decreasing mass accretion (Haiman & Menou 1999), a decreasing efficiency of the accretion (Cattaneo 1999), or a delayed quasar activity with respect to the dynamical formation of the halos, with a longer delay for smaller halos (Monaco et al. 1999).

As can be seen from Figure 17 of KH, the semianalytical models have difficulties in reproducing the steep decrease of the QSO density at low redshift that is commonly measured (Hartwick & Schade 1990). The most promising scenario is a ΛCDM, in which the accretion timescale, t_{acc}, is assumed to vary in the same way as the host galaxy dynamical time ($t_{acc} \propto [0.7 + 0.3(1 + z)^3]^{-1/2}$). This model is able to reproduce the evolution of the galaxy LF and of the cold gas content of galaxies, but it is apparently predicting a quasar decline that is too slow. The present data significantly reduce this disagreement in the sense that the higher quasar space density measured in our survey corresponds fairly well to the ΛCDM semianalytical predictions, as shown in Figure 5.

It is a pleasure to thank A. Wicenec for his invaluable help with the photometric database and F. La Franca, M. Haehnelt, and G. Kauffmann for enlightening discussions. We are indebted to Mira and Philippe Véron, whose indications helped us to improve significantly the accuracy of the identifications. We would also like to thank an anonymous referee for several useful comments that improved the paper. A. G. acknowledges the generous hospitality of ESO during two visits to Garching. This work is based on photographic data obtained using the UK Schmidt Telescope. The UK Schmidt Telescope was operated by the Royal Observatory Edinburgh, with funding from the UK Science and Engineering Research Council, until 1988 June, and thereafter by the Anglo-Australian Observatory. Original plate material is copyright by the Royal Observatory Edinburgh and the Anglo-Australian Observatory. The plates were processed into the present compressed digital form with their permission. The Digitized Sky Survey was produced at the Space Telescope Science Institute under US government grant NAG W-2166. The NASA/IPAC Extragalactic Database is operated by the Jet Propulsion Laboratory, California Institute of Technology, under contract with the National Aeronautics and Space Administration.

REFERENCES

Avni, Y., & Bahcall, J. N. 1980, ApJ, 235, 694
Banse, K., Ponz, D., Ounnas, C., Grosbol, P., & Warmels, R. 1988, in Instrumentation for Ground-Based Optical Astronomy, Present and Future, ed. L. B. Robinson (New York: Springer), 431
Boyle, B. J. 1992, in Ann. NY Acad. Sci., 647, Texas/ESO-CERN Symposium on Relativistic Astrophysics, Cosmology, and Particle Physics, ed. J. D. Barrow, L. Mestel, & P. Thomas, 14
Boyle, B. J., Shanks, T., Georgautopoulos, I., Stewart, G. C., & Griffiths, R. E. 1984, MNRAS, 271, 639
Burstein, D., & Heiles, C. 1982, AJ, 87, 1165
Cattaneo, A. 1999, preprint (astro-ph/9907335)
Cavaliere, A., Perri, M., & Vittorini, V. 1997, Mem. Soc. Astron. Italiana, 68, 27
Cristiani, S., et al. 1995, A&AS, 112, 347
Cristiani, S., & Vio, R. 1990, A&A, 227, 385
Franceschini, A., La Franca, F., Cristiani, S., & Martin-Mirones, J. M. 1994, MNRAS, 269, 683
Gehrels, N. 1986, ApJ, 303, 346
Goldschmidt, P., & Miller, L. 1998, MNRAS, 293, 107
Goldschmidt, P., Miller, L., La Franca, F., & Cristiani, S. 1992, MNRAS, 256, P65
Haiman, Z., & Menou, K. 2000, ApJ, 531, 42
Hartwick, F. D. A., & Schade, D. 1990, ARA&A, 28, 437
Hasinger, G., Burg, R., Giacconi, R., Schmidt, M., Trümper, J., & Zamorani, G. 1998, A&A, 329, 482
Hewett, P. C., & Foltz, C. B. 1994, PASP, 106, 113
Kauffmann, G., & Haehnelt, M. (KH) 2000, MNRAS, 311, 576
Köhler, T., Groote, D., Reimers, D., & Wisotzki, L. 1997, A&A, 325, 502
La Franca, F., & Cristiani, S. 1997, AJ, 113, 1517 (LC97)
La Franca, F., Franceschini, A., Cristiani, S., & Vio, R. 1995, A&A, 299, 19
Landolt, A. U. 1992, AJ, 104, 340
Lasker, et al. 1988, ApJS, 68, 1
Miyaji, T., Hasinger, G., & Schmidt, M. 2000, A&A, 353, 25
Monaco, P., Salucci, P., & Danese, L. 2000, MNRAS, 311, 279
Monet, D. 1996, A&AS, 188, 5404
Oke, J. B. 1990, AJ, 99, 1621
Omizzolo, A., Grazian, A., Cristiani, S., & Corbally, C. 2000, in preparation
Page, M. J., & Carrera, F. J. 2000, MNRAS, 311, 433
Schmidt, M., & Green, R. F. 1983, ApJ, 269, 352
Véron, M. P., & Véron, P. 1998, A Catalog of Quasars and Active Nuclei, ESO Scientific Report 18 (Munich: ESO) (VV98)
Voges, W. 1992, in Environment Observation and Climate Modelling Through International Space Projects: Space Sciences with Particular Emphasis on High-Energy Astrophysics (Noordwijk: ESA), 9–19 (RASS)
Voges, W., et al. 1999, A&A, 349, 389
Yuan, W., Siebert, J., & Brinkmann, W. 1998, A&A, 334, 498